Meteoritics & Planetary Science 41, Nr 4, 505–517 (2006)
Abstract available online at http://meteoritics.org

The Villalbeto de la Peña meteorite fall: II. Determination of atmospheric trajectory and orbit

Josep M. TRIGO-RODRÍGUEZ[1, 2*], Jiří BOROVIČKA[3], Pavel SPURNÝ[3], José L. ORTIZ[4], José A. DOCOBO[5], Alberto J. CASTRO-TIRADO[4], and Jordi LLORCA[2, 6]

[1]Institut de Ciències de l'Espai (ICE-CSIC), Campus UAB, Facultat de Ciències, Torre C-5, parells, 2a planta, 08193 Bellaterra (Barcelona), Spain
[2]Institut d'Estudis Espacials de Catalunya (IEEC), Ed. Nexus, Gran Capità 2-4, 08034 Barcelona, Spain
[3]Astronomical Institute of the Academy of Sciences, Ondřejov Observatory, Czech Republic
[4]Instituto de Astrofísica de Andalucía (IAA-CSIC), P.O. Box 3004, 18080 Granada, Spain
[5]Observatorio Astronómico Ramón Maria Aller, Universidade de Santiago de Compostela, Spain
[6]Institut de Tècniques Energètiques, Universitat Politècnica de Catalunya, Diagonal 647, 08028 Barcelona, Spain
*Corresponding author. E-mail: trigo@ieec.fcr.es

(Received 23 April 2005; revision accepted 3 November 2005)

Abstract–The L6 ordinary chondrite Villalbeto de la Peña fall occurred on January 4, 2004, at 16:46: 45 ± 2 s UTC. The related daylight fireball was witnessed by thousands of people from Spain, Portugal, and southern France, and was also photographed and videotaped from different locations of León and Palencia provinces in Spain. From accurate astrometric calibrations of these records, we have determined the atmospheric trajectory of the meteoroid. The initial fireball velocity, calculated from measurements of 86 video frames, was 16.9 ± 0.4 km/s. The slope of the trajectory was 29.0 ± 0.6° to the horizontal, the recorded velocity during the main fragmentation at a height of 27.9 ± 0.4 km was 14.2 ± 0.2 km/s, and the fireball terminal height was 22.2 ± 0.2 km. The heliocentric orbit of the meteoroid resided in the ecliptic plane (i = 0.0 ± 0.2°), having a perihelion distance of 0.860 ± 0.007 AU and a semimajor axis of 2.3 ± 0.2 AU. Therefore, the meteorite progenitor body came from the Main Belt, like all previous determined meteorite orbits. The Villalbeto de la Peña fireball analysis has provided the ninth known orbit of a meteorite in the solar system.

INTRODUCTION

The fall of the Villalbeto de la Peña meteorite (classified by Llorca et al. 2005 as an L6 chondrite) occurred in the north of the province of Palencia, Spain, on Sunday, January 4, 2004 at 16:46:45 ± 2 s UTC. The fireball associated with this fall appeared in broad daylight when thousands of people were attending various festivities in the northern part of the Iberian Peninsula. More than one hundred eyewitness reports of the bolide arrived from sites located as much as 600 km away or more. The increasing availability of digital photography and video cameras makes it possible for casual eyewitnesses to obtain valuable records of daylight fireballs. We were able to obtain from the eyewitnesses one video record and two photographs of the fireball's flight (Figs. 1 and 2). After the fireball's disappearance, a 25 ± 1 km long, smoky trail remained visible at the end of the trajectory for ~35 min (Fig. 3). This is important because several people photographed the persistent train a few seconds after the fireball from various perspectives. The fireball's observations and records were compiled in the framework of the Spanish Meteor Network (SPMN), with the valuable collaboration of several astronomical associations, allowing us to obtain an extraordinary amount of valuable data. Under this framework, we obtained from the Villalbeto de la Peña fall nearly a hundred visual reports, dozens of pictures, and one video record (Fig. 4). Llorca et al. (2005) presented information on the energy released in the atmosphere by this fireball, deduced from video, seismic, and infrasound data, together with information on the meteorite recovery, classification, isotopic analysis, and petrography. In this paper, we focus on the determination of the fireball's atmospheric trajectory and the determination of the heliocentric orbit of the progenitor body. We also develop a dynamic model of the fireball's flight in order to model the dark flight of the meteorite fragments and estimate the initial velocity of the body during atmospheric entry.

© The Meteoritical Society, 2006. Printed in USA.

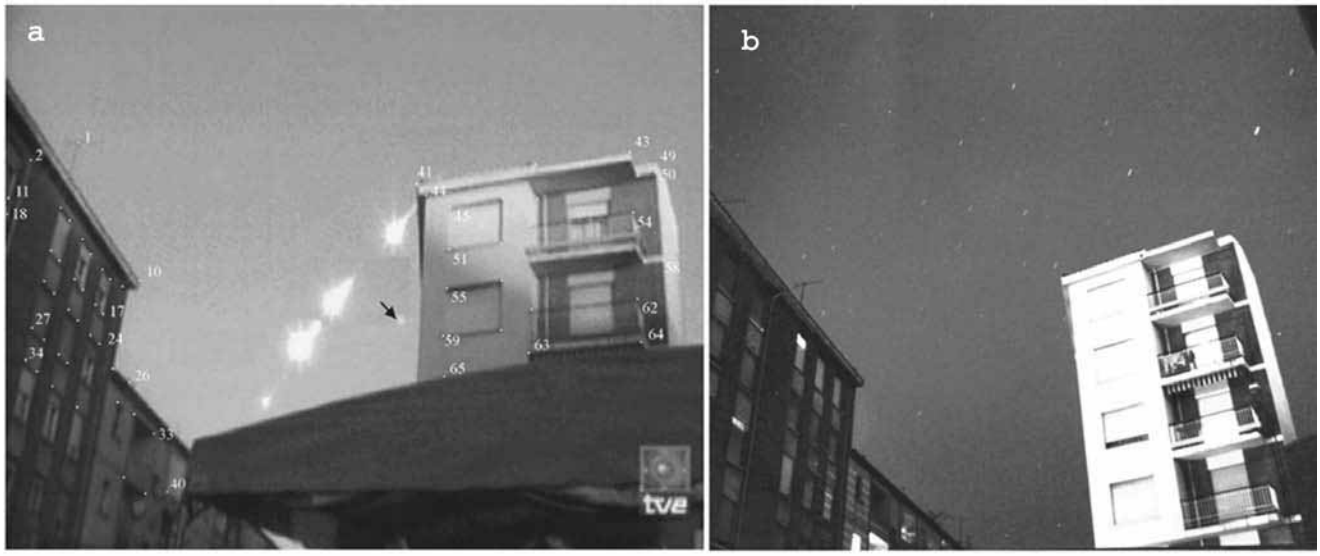

Fig. 1. a) A composite image of the video record in selected frames where the 65 calibration points measured in every frame have been identified. A temporal sunblind is visible at the bottom of the picture. b) One of the calibration pictures containing stars from the constellations Boötes, Hercules, and Draco. Video courtesy of Televisión Española.

TRAJECTORY DATA

From the detailed study of the daylight bolide associated with this fall, we have determined the atmospheric trajectory, velocity, and orbit of the incident body. In order to estimate trajectory data, we have used the video record (Figs. 1a and 2c), two direct photographs of the fireball (Figs. 2a and 2b), and one picture of the persistent train (Fig. 3f). We made detailed stellar calibrations for the video and the three photographic records with horizon details in a similar way as did Borovička et al. (2003) for the Morávka meteorite fall. Basically, stellar calibration pictures were taken from the different locations where the fireball was fortuitously recorded. As the method requires knowing the position of the cameras with great precision, in some cases several attempts were required to find the exact position where the original pictures were taken. Identification of common points in both the original and the calibration images was made. In a subsequent step, we obtained the astrometric positions of the stars in the calibration picture and measured the apparent coordinates of common objects in the original and calibration pictures. By using them, we determined the azimuth and elevation of the fireball. In the case of the video record, this procedure was applied to every single frame. The almost-full Moon was recorded on the video record and the Santa Columba pictures simultaneously with the fireball. The Moon's position could therefore be used for the final refinement of the calibration.

The location of the different stations and some additional data are shown in Table 1. Additional pictures of the fireball's train provided information on the fragmentation processes that occurred along the last part of the fireball trajectory (Fig. 3). One picture taken from Guardo suggests that at least two big fragments survived the main fragmentation event occurring at 24 km, leaving parallel dust trains (Fig. 3a). This observation is consistent with the multiple fragments that were photographed in flight from Santa Columba de Curueño (Figs. 2b and 2d).

From the data collected in situ, we discuss some of the closest reports to the fireball that provide additional information on the audibility of the sonic boom produced mainly during the atmospheric breakup of the meteoroid. Figure 4 collects all available audio data, although is important to note that the distribution of reports was nonuniform as a consequence of the low population of some areas. The energy of the explosion, derived from additional seismic and infrasound data, was given in Llorca et al. (2005). A huge explosion followed by a noise like that of drums or rolling thunder was heard, mainly in a region of ~50 km around the fragmentation point, but curiously some reports were obtained from sites adjacent to the earlier parts of the meteor trajectory. An example is the audio witnesses located in Mansilla or Sahagún, approximately ~70 km in front of the fragmentation point. These sounds may either have been generated at the earlier parts of the trajectory and propagate perpendicularly to the trajectory or may represent sonic booms generated at point-like fragmentation explosion near the end of the trajectory, initially propagating upward and then reflected from upper atmosphere.

From the calibration of video and photographs, we computed the fireball trajectory by the method of Borovička (1990). The trajectory projected on the ground is plotted in Fig. 5. The meteoroid hit the atmosphere from the southwest, with a slope relative to the Earth's surface of 29.0 ± 0.6°,

Fig. 2. Selected images of the fireball. a) An image of the fireball after the first seconds of flight taken from Las Oces de Valdeteja (León) by Salvador Díez. The fireball was at a height of 43 km at that moment. b) A photograph obtained from Santa Columba de Curueño (León) by Maria M. Robles. This image was taken just after the main fragmentation event, showing several pieces in flight. c) A video frame obtained by Luís A. Fernández and Carmen Blanco of the exact moment of its flight imaged in Fig. 2b. Photograph courtesy of Televisión Española. d) A magnification of (b) showing the different points identified on the video frame. All of these images were used for calibration. The bright spot in images (b), (c), and (d) is the Moon.

resulting in a visible fireball path 130 ± 10 km long (assuming the beginning height between 80–90 km). The trajectory data is given in Table 2. The videotape recorded various explosions along the meteoroid's trajectory, with the largest (main) fragmentation occurring at an altitude of 27.9 ± 0.4 km. All these explosions are also easily identified in the pictures of the fireball in flight (Figs. 2c and 2d). Amazingly, the resolution shown in Fig. 2d makes it possible to see the dust-vapor cloud associated with the main fragmentation event, the main body producing the fireball's head, and some small fragments flying behind the main body. Unfortunately, the video resolution was not sufficient to resolve individual fragments except for a few frames after the main fragmentation. Consequently, it was not possible to estimate their velocity and deceleration. The largest fragment maintained higher velocity and continued its flight, producing light until a height of at least 22 km above the terrestrial surface. The smallest ones were losing velocity and delayed in flight, and the prevalent wind direction could make them land southeast of the trajectory. The relatively small slope of the trajectory and the numerous fragmentation events at different heights contributed to the dispersion of the meteorites over a large area. The meteorite distribution in the strewn field of about 95 km^2 is consistent with this scenario (Llorca et al. 2005). To predict the impact point of the largest meteorite fragment and to infer the heliocentric orbit of the meteoroid, a fireball velocity solution was necessary. This was possible using the video record.

FIREBALL VELOCITY AND FRAGMENTATION

Eighty-six positional measurements of the fireball, covering the time interval of 1.70 s with the resolution of 0.02 s, were obtained from the video record. The record

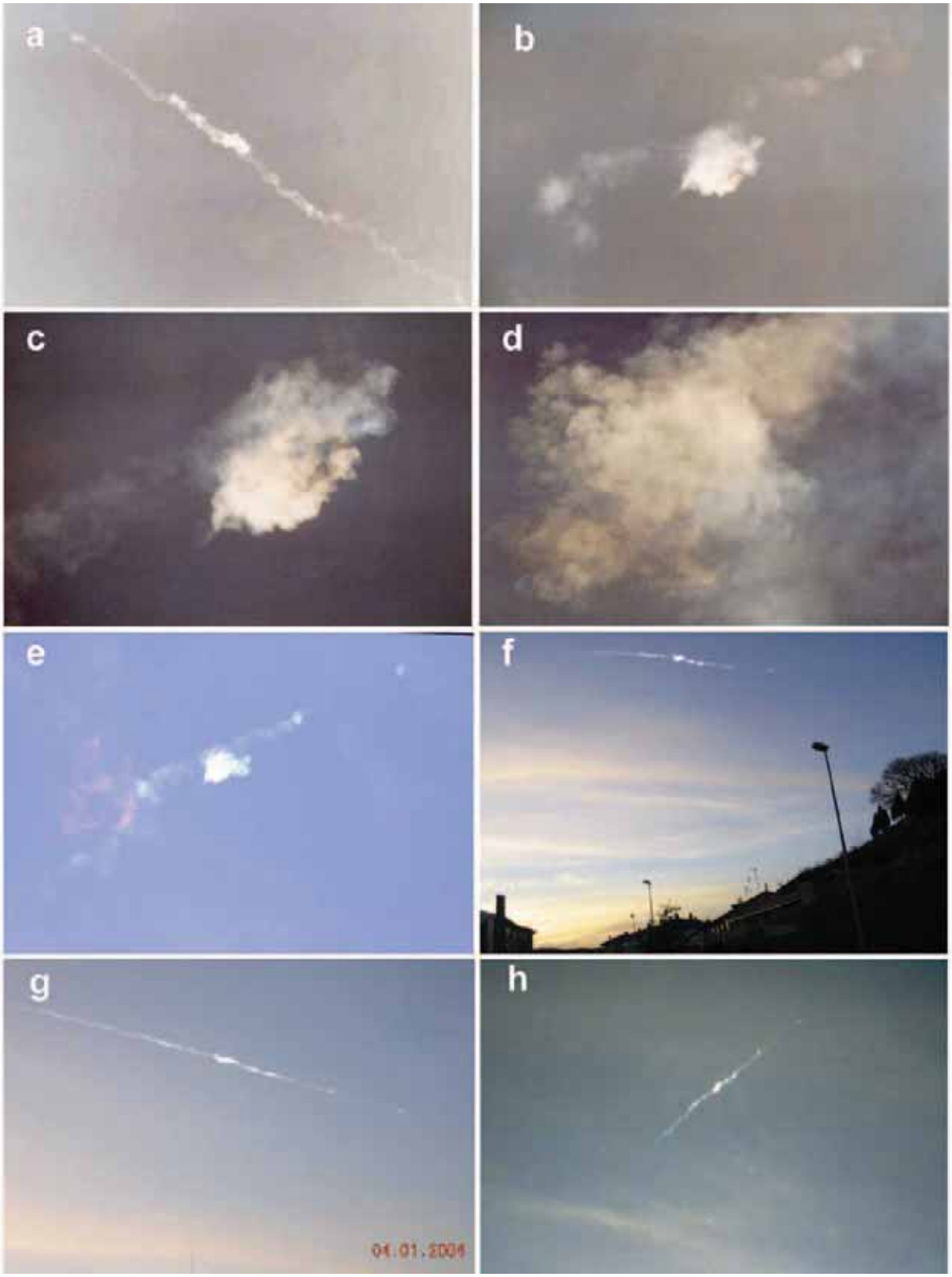

Fig. 3. Selected images of the persistent train. Several fragmentation events are associated with various dense vapor clouds. a–d) A sequence of images obtained from Guardo by Eugenio Aparicio. e) An image obtained by Jesús Martín from Villalbeto de la Peña, the locality where the first meteorites were recovered a few days later. f) An image used for calibration purposes taken from Aguilar de Campoo by Raúl Varona. g) An image obtained by Rubén Rodríguez from Valdecastro. h) An image from Ruesga taken by María A. Fernández.

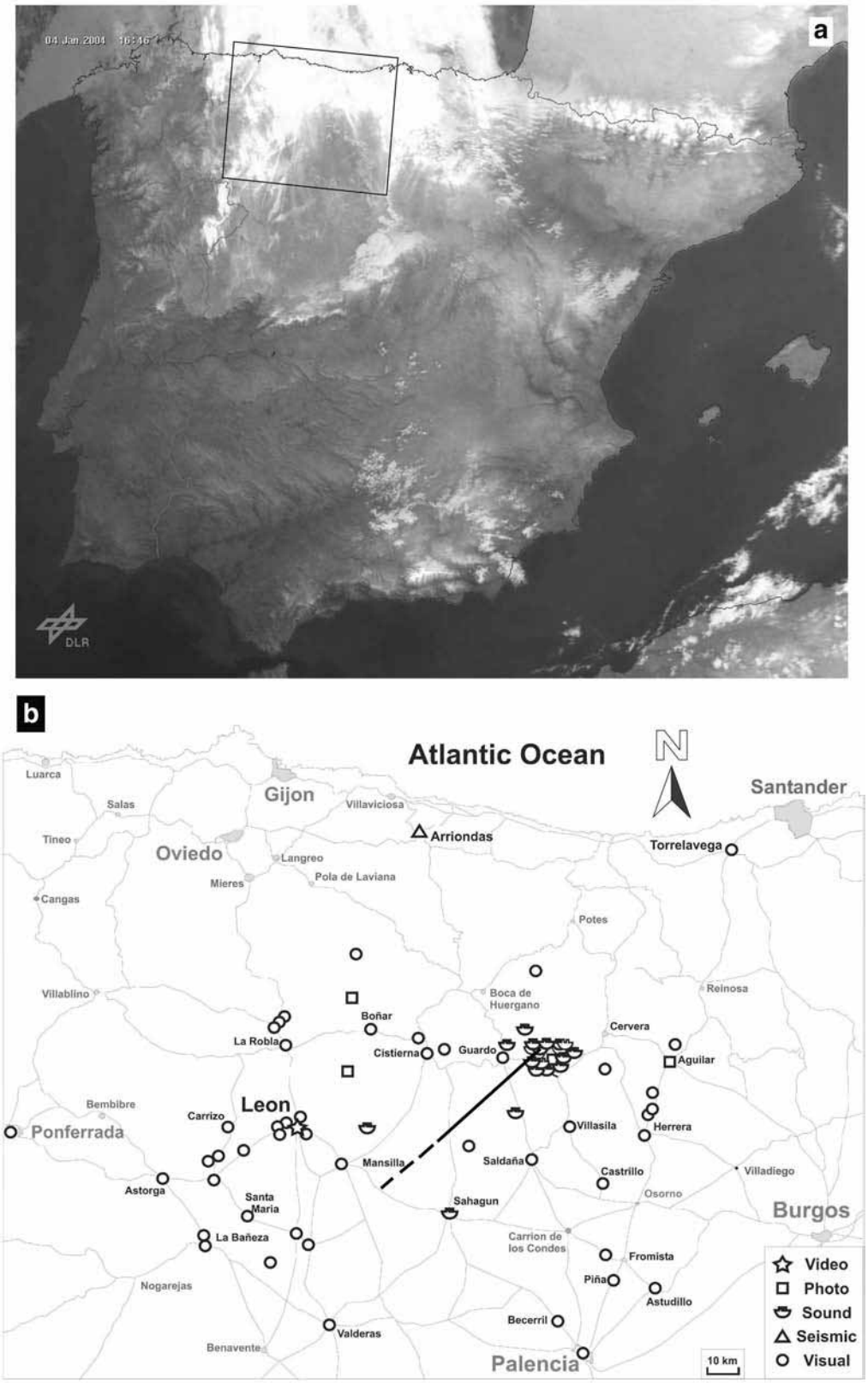

Fig. 4. a) An NOAA image showing the weather conditions on January 4, 2004, at 16:46 UTC. The box in the image outlines the region shown in the map below. b) A detailed map of the region overflown by the fireball showing all reported observations: video, photographic, sound, seismic, and visual.

Table 1. Details of the video and photographic records of the Villalbeto de la Peña fireball.

Site	Longitude (°W)	Latitude (°N)	Altitude (m)	Field of view (°)	Record length (s)	No. of positions (head/train)	Image format
León	5.55942	42.59792	821	44 × 27	1.74	86/0	MiniDV
Las Oces (León)	5.39594	42.90178	1080	32 × 22	0.01	1/11	Digital
Santa Columba de Curueño (León)	5.40181	42.74628	915	34 × 20	>1	1/7	Color negative
Aguilar de Campoo (Palencia)	4.26106	42.79589	884	50 × 9	Train	0/20	Digital

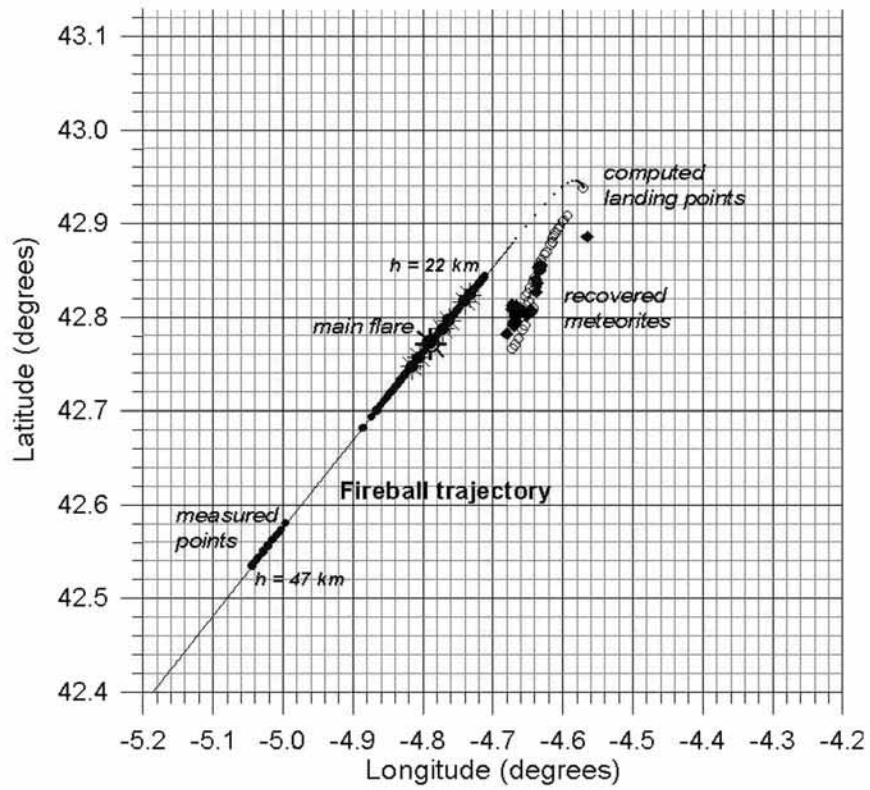

Fig. 5. The terminal part of the trajectory of the Villalbeto de la Peña fireball projected on the ground. Filled circles show the measured points along the trajectory. Large circles with asterisks indicate the positions of the observed flares. Full diamonds show the positions of the recovered meteorites. Computed landing points of possible meteorites are indicated by empty circles. The step of 0.1 degree in latitude corresponds approximately to 11 km on the ground.

contains the brightest part and the final part of the fireball, from a height of 32.8 km to the fireball disappearance at a height of 22.2 km. The measurement of the length along the trajectory as a function of time provides us with the information on fireball velocity. The individual measurements, however, are affected by large measurement errors, and the point-to-point velocity shows enormous scatter. A physically reasonable fit to the data is necessary. The motion of a single ablation meteoroid is governed by well-known equations of meteor physics (e.g., Ceplecha et al. 1998). Provided that the initial mass, velocity, ablation coefficient, and shape-density coefficient are known, the deceleration and mass-loss of a meteoroid can be computed. In reality, the situation is complicated by fragmentation events, where mass decreases abruptly.

The fireball light curve obtained from the video record and the dynamic model are compared in Fig. 6. The light curve shows that at least seven major fragmentations occurred within the covered interval. We have taken the positions of the fragmentation derived from the light curve as fixed. Between the fragmentations, the meteoroid was treated as a single body. The ablation coefficient was assumed to be $0.003\ s^2\ km^{-2}$ in accordance with the findings for the Morávka fireball (Borovička and Kalenda 2003). The density of the meteoroid was set equal to the density of the recovered meteorites, i.e., $3.42\ g\ cm^{-3}$ (Llorca et al. 2005). The ΓA, where Γ is the drag coefficient and A is the shape coefficient, was assumed to be $\Gamma A = 1.0$. We had therefore to determine the initial velocity and mass and the amount of mass loss in each fragmentation. This was done by fitting the fireball

Table 2. Atmospheric trajectory data of the Villalbeto de la Peña meteorite fall. The length of the recorded trajectory (from the first measured point at Las Oces to the end of video record) is 50 km. This covers the heights from 47 km to 22 km.

	Beginning	Main fragmentation	Terminal
Velocity (km/s)	16.9 ± 0.4	14.2 ± 0.2	7.8 ± 0.3
Height (km)	–	27.9 ± 0.4	22.2 ± 0.4
Longitude W (°)	–	4.789	4.711 ± 0.006
Latitude N (°)	–	42.771	42.8437 ± 0.002
Dynamic mass (kg)	600 ± 200	–	10 ± 5
Slope (°)	29.0 ± 0.6		
Azimuth (°)	38.6 ± 1.3		
Total trajectory length (km)	130 ± 10 (recorded ~50)		
Maximum absolute magnitude	−18 ± 1		

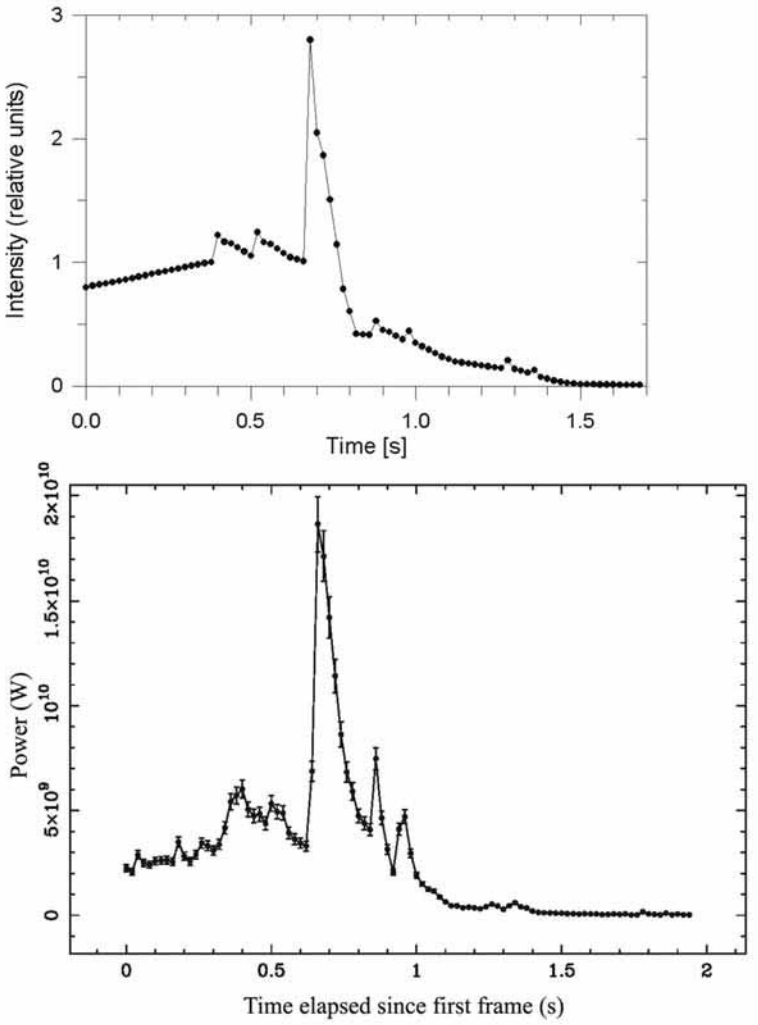

Fig. 6. A simulated light curve of the fireball (top) for comparison with the observed light curve (bottom). The observed light curve is adapted from Llorca et al. (2005).

dynamics, i.e., the observed length as a function of time. The equations given in Ceplecha et al. (1998) were used, and the free parameters were adjusted manually in a similar way as was done for the Morávka fragments (Borovička and Kalenda 2003).

The best fit gave the velocity and mass at the beginning of the video record of 15.5 ± 0.2 km s^{-1} and 550 ± 150 kg, respectively. The course of the velocity and mass along the trajectory is given in Fig. 7. The velocity decreased to 7.8 km s^{-1} at the end of the video record and the nominal mass at that point was 13 kg. In our model, the mass decreased from 450 kg to 130 kg in the main fragmentation event at the height

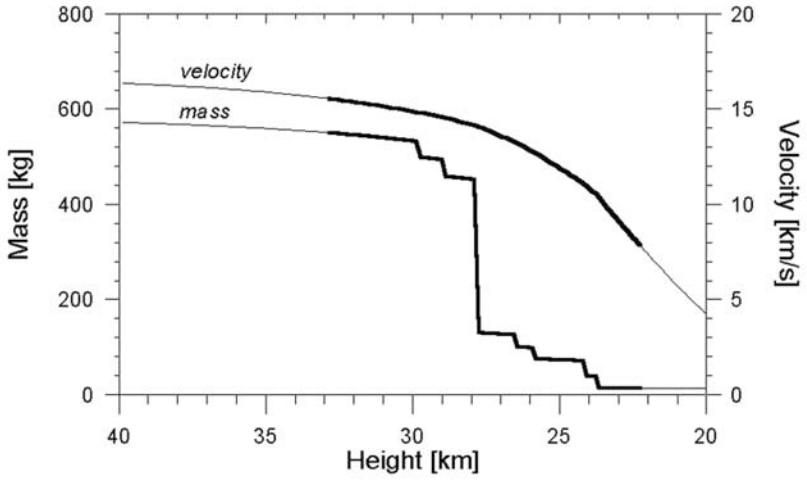

Fig. 7. The modeled mass and velocity of the main body of the Villalbeto fireball as a function of height in the atmosphere. The part of the trajectory covered by video observation is plotted with thick line. The thin line is an extrapolation.

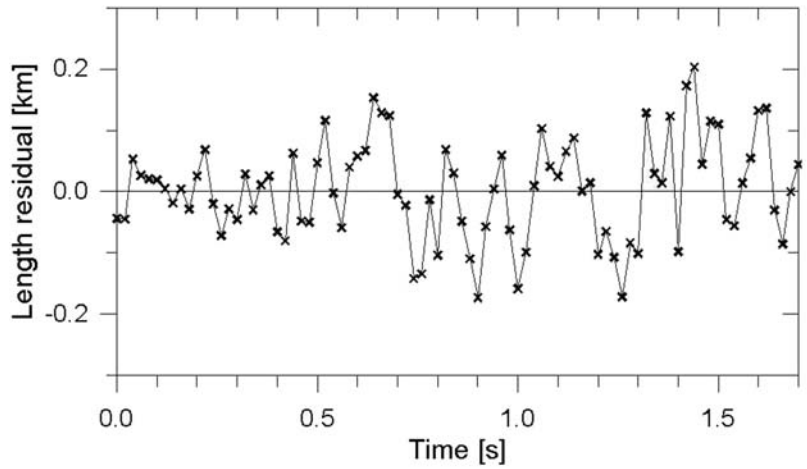

Fig. 8. The fit of fireball dynamics. The differences between the lengths along the trajectory measured on 86 video frames and the lengths computed from the fragmentation model are plotted as a function of time.

of 27.9 km. The maximal dynamic pressure experienced by the meteoroid was 5 MPa, very similar to the Morávka case (Borovička and Kalenda 2003).

The quality of the fit is demonstrated in Fig. 8. There is almost no systematic trend in the residua; the differences between the observed and computed lengths are random and can be attributed to the measurement errors. Another check of the model is possible by computing the simulated light curve. In accordance with the classical theory, the intensity of the emitted radiation was assumed to be proportional to the loss of kinetic energy of the meteoroid. After fragmentation, all released mass was assumed to be radiated out within the next 0.12 s, causing the meteor flare. The simulated and observed light curves are very similar, as we can see in Fig. 6. Although there are some differences, in particular in the amplitudes of the flares, we consider the agreement as satisfactory.

ORBITAL DATA

To compute the heliocentric orbit of the Villalbeto meteoroid, we needed to know the pre-atmospheric velocity of the body. At a height of 33 km, where the video record begins, the body had already been decelerated by the atmospheric drag. We estimated the original velocity at a height of 90 km by extrapolating the dynamic data obtained in the previous section backwards. We assumed that no significant fragmentation occurred before the start of the video record. This may be or may not be true. The Morávka fireball was shown to have experienced severe fragmentation above the height of 50 km (Borovička and Kalenda 2003). Without fragmentation, the extrapolation yielded the original velocity of 16.9 km s^{-1}. Taking all uncertainties into account, the standard deviation of this value is not smaller than ±0.4 km s^{-1}. The extrapolated initial dynamic mass is 600 ±

Table 3. Orbital data of the progenitor body of the Villalbeto de la Peña L6 chondrite (epoch of the fall J2004.01).

	Villalbeto de la Peña
Apparent right ascension (°)	317.2 ± 1.2
Apparent declination (°)	–9.9 ± 0.4
Initial velocity (km/s)	16.9 ± 0.4
Geocentric right ascension (°)	311.4 ± 1.3
Geocentric declination (°)	–18.0 ± 0.7
Heliocentric velocity (km/s)	37.7 ± 0.5
T (Epoch of perihelion passage)	2003 Dec 2 ± 1 day
Eccentricity	0.63 ± 0.04
Semimajor axis (AU)	2.3 ± 0.2
Inclination (°)	0.0 ± 0.2
Argument of perihelion (°)	132.3° ± 1.5[a]
Longitude of the ascending node (°)	283.6712°[a]
Orbital period (yr)	3.5 ± 0.5
Perihelion distance (AU)	0.860 ± 0.007
Aphelion distance (AU)	3.7 ± 0.4
Longitude of perihelion (°)	56.0° ± 1.5°

[a] Valid for $i > 0$, otherwise shift by 180°.

200 kg. This is in reasonable agreement with the radioisotope analysis, which gave 760 ± 150 kg (Llorca et al. 2005), and indicates that no severe fragmentation occurred in the early part of the trajectory.

The resulting orbital elements are given in Table 3. Within the error limits, the inclination is zero. For zero inclination, the longitude of the ascending node, Ω, is not defined. Nevertheless, the inclination was surely not exactly zero and we may set the longitude of the ascending node equal to the longitude of the Sun at the time of the fireball appearance (this assumes that the meteoroid encountered Earth in the ascending node, which seems to be more probable; in the opposite case, Ω would be lower by 180°). Computing the precession, i.e., re-computing Ω and the argument of perihelion, ω, to a standard epoch is, however, not possible for inclination of zero. The elements in Table 3 are therefore given for the epoch of the fireball, i.e., 2004.01.

The heliocentric orbit of the Villalbeto meteoroid is similar in character to the other eight meteorites with known orbits (Table 4; Fig. 9). It is an Apollo-type orbit with its aphelion lying in the Main Belt. Unfortunately, the uncertainty of the fireball initial velocity transforms strongly into the uncertainty in the semi-major axis, which is about 10%.

DARK FLIGHT AND METEORITE IMPACT

The fireball dynamical data can also be extrapolated forward in order to predict the impact point of the largest meteorite fragment. At the end of the video record, the fireball velocity was 7.8 ± 0.3 km s^{-1}. At this moment, the fireball luminosity decreased below the limit of the video camera in daylight. Nevertheless, it is known from more sensitive nighttime observations that fireballs radiate—and the ablation therefore proceeds—until the velocity decreases to 3–4 km s^{-1} We therefore extrapolated the ablation phase until the modeled velocity decreased to 4 km s^{-1}. This occurred at a height of 20 km; the computed mass of the meteoroid at that point was 12 kg. From there, the standard dark flight computation (Ceplecha et al. 1998) was performed. The atmospheric wind field as provided by the Instituto Nacional de Meteorología is presented in Fig. 10. The wind from westerly to northerly directions prevailed and reached the maximum speed of 45 m s^{-1} at the height of 13 km.

The nominal coordinates of the impact point are 4.570°W and 42.937°N. The point is plotted in Fig. 5 as the northernmost meteorite. It lies 14 km (as measured on the ground) behind the video terminal point and is shifted by the winds 2 km to the southeast from the trajectory prolongation. However, we must note that the computation assumes that no fragmentation occurred near the end of the video trajectory or after that. The existence of a well-defined small cloud at the end of the fireball train (Fig. 3) at a height of 22 km suggests that a sudden mass loss occurred. In that case, the main meteorite would lie closer to the trajectory end. It cannot even be excluded that the meteoroid was separated into two or more pieces and no single big meteorite exists. The nominal mass of 12 kg is an upper limit, not only because additional fragmentation may have occurred, but also because it was computed for $\Gamma A = 1.0$. If the correct A value was 0.8, as suggested by Borovička and Kalenda (2003) for the Morávka case, the nominal mass would be 6 kg.

To date, 33 meteorites ranging in mass from 11 g to 1.4 kg were recovered: 32 meteorites that were reported by Llorca et al. (2005), and one additional 0.562 kg specimen that was found by a German finder in May 2005 at the position 4.63204°W, 42.85488°N, h = 1425 m. The positions of the meteorites are also plotted in Fig. 5. It is obvious that these meteorites were separated from the main body in the various fragmentation events along the trajectory. We have therefore tried to simulate the flight of fragments produced in the seven known fragmentation events, which occurred between the heights of 30 km and 23.5 km. Five fragments with the masses of 3 kg, 1 kg, 300 g, 100 g, and 30 g were launched at each fragmentation point with the velocity of the fireball at that point and in the same direction as the main body. One 3 kg body was also launched from the fireball terminal point (as seen on the video). The ablation model was applied until the velocity decreased to 4 km s^{-1}; the dark flight was computed after that. The fragments are expected to lose 10–30% of their original mass during the ablation phase (the highest value is valid for the fragments originating at the highest altitude). The computed landing points are plotted in Fig. 5. There is a good overlap with the meteorite specimens that were actually recovered, which justifies the reliability of the inferred fireball trajectory. The only significantly

Table 4. Main orbital data of recovered meteorites. References are: 1) Ceplecha (1961); 2) Spurný et al. (2003); 3) Grady (2000); 4) McCrosky et al. (1971); 5) Halliday et al. (1978); 6) Brown et al. (1994); 7) Brown et al. (2002b); 8) Borovička et al. (2003); 9) Brown et al. (2004); 10) Llorca et al. (2005); 11) this work.

Meteorite name	Year of fall	Recovered mass	Meteorite type	Orbital data			
				a (AU)	e	i (°)	References
Příbram	1959	5.8	H5	2.401 ± 0.002	0.6711 ± 0.0003	10.482 ± 0.004	1, 2, 3
Lost City	1970	17	H5	1.66 ± 0.01	0.417 ± 0.001	12.0 ± 0.1	4
Innisfree	1977	4.58	L5	1.872 ± 0.001	0.4732 ± 0.0001	12.27 ± 0.01	5
Peekskill	1992	12.57	H6	1.49 ± 0.03	0.41 ± 0.01	4.9 ± 0.2	6
Tagish Lake	2000	5–10	CI?	2.1 ± 0.2	0.57 ± 0.05	1.4 ± 0.9	7
Morávka	2000	1.4	H5–6	1.85 ± 0.07	0.47 ± 0.02	32.2 ± 0.5	8
Neuschwanstein	2002	6.2	EL6	2.40 ± 0.02	0.670 ± 0.002	11.41 ± 0.03	2
Park Forest	2003	18	L5	2.53 ± 0.19	0.680 ± 0.023	3.2 ± 0.3	9
Villalbeto de la Peña	2004	~5	L6	2.3 ± 0.2	0.63 ± 0.04	0.0 ± 0.2	10, 11

deviating fragment is the largest one. The 1.4 kg meteorite sample lies 3.5 km off the predicted meteorite line. Of course, in reality, the meteorite line is widened into the fall ellipse by random impulses that the meteorite fragments gain during the fragmentation by aerodynamic effects during the dark flight, and by other influences. We therefore still consider the agreement as satisfactory, but we expect other possible meteorite fragments of similar mass to be located several kilometers to the west from the 1.4 kg piece.

CONTRIBUTION OF THE VILLALBETO DE LA PEÑA FALL TO WELL-KNOWN METEORITE ORBITS

In recent years, an increasing appreciation for the hazards posed by near-Earth objects (NEOs) has appeared, coinciding with increasing coverage of these objects (Rabinowitz et al. 1993, 2000; Bottke et al. 2000, 2004; Carusi et al. 2002; Stuart and Binzel 2004). The smallest population of these bodies is formed by objects a few tens of meters in diameter, whose detection is made possible only by wide-field telescopes when these objects are in near-Earth space or when they produce a superbolide in the terrestrial atmosphere. These events are usually associated with bodies with masses greater than 1000 kg, corresponding to a size range between 0.1 to several tens of meters (Ceplecha 1996). The biggest events detected by fireball networks are usually produced by bodies with a mass close to 10 kg (Halliday et al. 1996; Steel 1996), although some larger events also occur (Borovička and Spurný 1996; Spurný et al. 2003). A major problem is the lack of knowledge of the size distribution of NEOs at small diameters. Particularly, the size range between about one meter to some tens of meters constitutes the least-known objects of the solar system; nevertheless, they are easily detectable from ground networks or satellites during the bolide phase because they produce events with energy in the range between 10^{-2} and 10^{4} kt of TNT (Di Martino and Cellino 2004). The energy released during the Villalbeto de la Peña event was estimated to be 2×10^{-2} kt from photometric, seismic, and infrasound data, corresponding to a meteoroid 0.7 m in size (Llorca et al. 2005). Following the distribution of impactors given by Brown et al. (2002a), the Earth receives ~10 impacts with such energy every month.

The success of obtaining an accurate reconstruction of the original orbit in the solar system of a meteorite has been obtained on nine occasions (Table 4). Among these cases, six meteorites are ordinary chondrites: Příbram, recovered in Czechoslovakia in 1959 (Ceplecha 1961); Lost City, recovered in the USA in 1970 (McCrosky et al. 1971); Innisfree, recovered in Canada in 1977 (Halliday et al. 1978); Peekskill, recovered in the USA in 1992 (Brown et al. 1994); Morávka fall, which occurred in the Czech Republic in 2000 (Borovička et al. 2003); Park Forest, which occurred in suburban Chicago, USA in 2003 (Brown et al. 2004); and Villalbeto de la Peña, Spain in 2004 (this work). Two more recent falls have provided information about other meteorite types. The first one was the unique carbonaceous chondrite fall of Tagish Lake, which occurred in Canada in 2000 (Brown et al. 2002b). The second one occurred in Neuschwanstein (Germany) in 2002, where an enstatite chondrite was recovered (Spurný et al. 2003). In addition, fifteen much less accurate orbits have been derived from visual observations (Wylie 1948; La Paz 1949; Fesenkov 1951; Krinov 1960; Folinsbee et al. 1969; Levin et al. 1976; Ballabh et al. 1978; Brown et al. 1996; Halliday and McIntosh 1990; Jenniskens et al. 1992; Gounelle et al. 2006). Considering that the number of reported falls and known meteorites until 1999 was respectively 1005 and 22,507 (Grady 2000), we can conclude that our knowledge on the origin of these objects is very limited. In fact, orbital data are available for only ~1% of the observed falls and less than 1‰ of all recovered meteorites. It is necessary to increase the number of reported cases by making a special effort to compile all valuable observations for each fireball event.

In Table 4, the orbits of progenitor bodies of recovered meteorites are compiled. To date, all of these bodies have

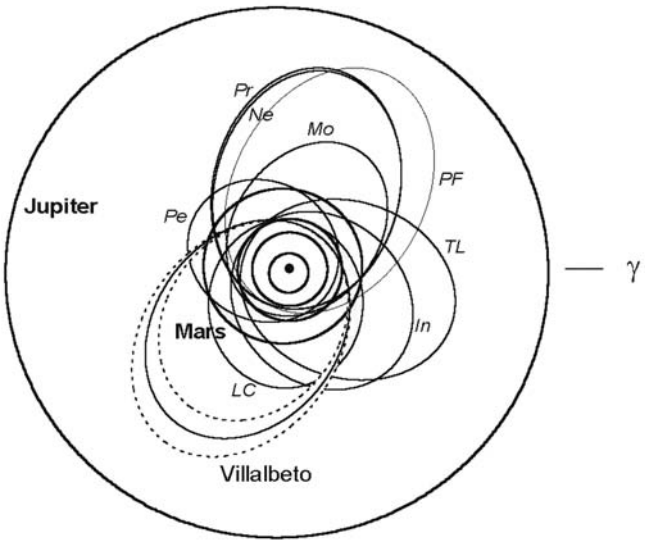

Fig. 9. The orbit of the Villalbeto de la Peña progenitor body (including the uncertainty) compared to previously determined orbits of meteorites. The projection to the ecliptic plane is shown. Vernal equinox is to the right.

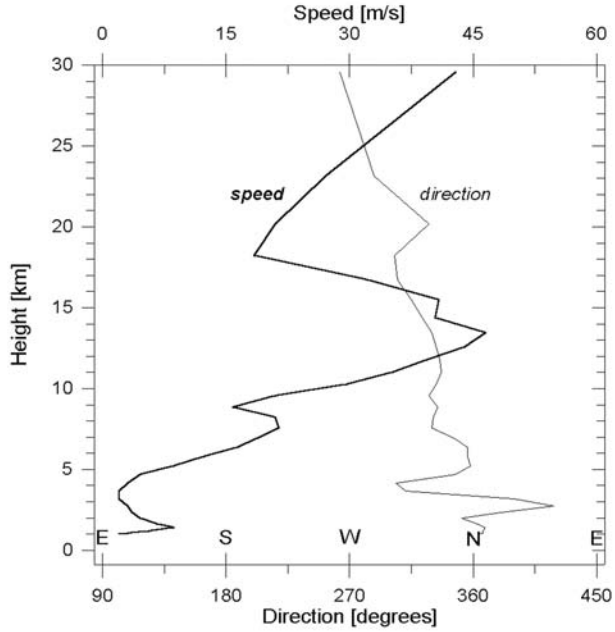

Fig. 10. The vertical profile of the horizontal mean wind speed at longitude −5.2° and latitude 42.8° on January 4, 2004, 18:00 UT. Source: The HIRLAM model, Instituto Nacional de Meteorología.

come from the Main Belt. Part of the orbits have semimajor axes of ~2.5 and eccentricities of ~0.6. By looking at the similitude between these two orbital elements, it seems that Příbram, Neuschwanstein, Park Forest, and Villalbeto de la Peña were delivered to the Earth by the 3/1 main jovian resonance (Wisdom 1985a, 1985b). However, other diffusive resonances can also be participating in the delivery of meteorites to the Earth (Gladman et al. 1997; Morbidelli and Gladman 1998). Once a body has been perturbed into the Mars-crossing region, the effect of Martian encounters can send these objects to a resonance strong enough to cause a further decrease in their perihelion. In such a way, Mars-crossing meteoroids can enter in the NEO region where they spend a mean time of 3.75 Myr (Bottke et al. 2002). For example, Lost City and Peekskill had semi-major axes close to Mars' orbit. In fact, by using the source-region model for NEAs of Bottke et al. (2002) and taking into account the uncertainties in the orbital elements, we find that Villalbeto de la Peña could have originated in one of four regions: the 3:1 jovian resonance, the ν_6 resonance, the Mars-crossing region,

and the outer Main Belt (OMB). The probability associated with the OMB source is surprisingly high for the orbit of a meteorite. In fact, the probability distributions in Bottke et al. (2002) indicate that the OMB source has a "finger" at low inclination that the other sources lack (Bottke 2005). Despite this interesting feature, the derived similar probabilities for the four different sources make it difficult to determine the exact source of Villalbeto de la Peña. However, we should remark that the Yarkovsky effect is not considered in the Bottke et al. (2002) computations although it is expected to affect the dynamics of meteoroids 1 m in size (Vokrouhlický and Farinella 2000).

CONCLUSIONS

The Villalbeto de la Peña fireball represents another valuable instance of accurate determination of the origin of a recovered meteorite. The origin of the progenitor body is located in the Main Belt ($a = 2.3 \pm 0.2$ AU, $e = 0.63 \pm 0.04$, $i = 0.0 \pm 0.2°$). The analysis of the data gathered on the speed, luminosity, sound phenomena, penetration of the material in the atmosphere, and the persistent train, as well as the detailed analysis of the meteorite itself, has converted the Villalbeto de la Peña meteorite fall into one of the best documented in history.

Acknowledgments–We are grateful to the Ministerio de Educacion y Ciencia (MEC 2004-20101-E) for financial support. The work of Czech co-authors was supported by the project AV0Z10030501. J. M. T.-R. is grateful to the Spanish State Secretary of Education and Universities for a postdoctoral grant. We thank Drs. Bartolomé Orfila and Juan Guerra Gómez of the Instituto Nacional de Meteorología for atmospheric profiles. Saúl Blanco, Ricardo Chao, and Manuel Fernández of the Asociación Leonesa de Astronomía together with Óscar Díez and Stanislaus Erbrink of the Agrupación Astronómica Palentina participated in the calibration of the original images of the fireball. Fig. 4b was kindly drawn by Dr. Javier García-Guinea (Museo Nacional de Ciencias Naturales-CSIC). The Agrupación Astronómica Cántabra, the Agrupación Astronómica de Madrid, and SOMYCE participated in collecting additional data. Eyewitnesses and collaborators who provided valuable data are: Noelia Arroyo, Vicente J. Ballester, Javier Benedit, Orlando Benítez, Natalia Calle, Josep Cruz, Adolfo Delibes, Montse Guiu, Manuel Iglesias, José I. Cuende, Sergio Dalmau, Alvaro Faraco, Vicent Favà, Jesús Fernández, Pere-Miquel Fonolleda, Magí Fonolleda, Fernando Fontenla, Francisco Galindo, Francisco M. Garrido, Olga Guasch, Vicente Guisasola, Montse Guiu, Jaime Izquierdo, María José Marín, Jesús Martín, Enrique Neira, Francisco Ocaña, Ramón Pallarés, Lorena Pardinas, Joan Peñalver, José M. Pérez, Silvia Pérez, Carles Pineda, Alejandro Polanco, Ramon Puigneró, Miquel Rafa, María M. Robles, Oscar A. Rodríguez, Jesús San-José, Albert Sánchez, Mari C. Sobrinos, Joaquín Tapioles, Jordi Tapioles, Jordi Torra, Raul Varona, Jordi Xifré, and others who prefer to be anonymous. We also thank the finder who provided us with the weight and location of the 33rd specimen of Villalbeto de la Peña, who prefers to remain anonymous. We are indebted to Luís A. Fernández-Arenas, Carmen Blanco, and Televisión Española for providing us with the original video, and to the authors of the pictures of the fireball and its persistent train, listed in Figs. 2 and 3.

Editorial Handling—Dr. Donald Brownlee

REFERENCES

Ballabh G. M., Bhatnagar A., and Bhandari N. 1978. The orbit of the Dhajala meteorite. *Icarus* 33:361–367.

Borovička J. 1990. The comparison of two methods of determining meteor trajectories from photographs. *Bulletin of the Astronomical Institute of Czechoslovakia* 41:391–396.

Borovička J. and Kalenda P. 2003. The Morávka meteorite fall: 4. Meteoroid dynamics and fragmentation in the atmosphere. *Meteoritics & Planetary Science* 38:1023–1043.

Borovička J., Spurný P., Kalenda P., and Tagliaferri E. 2003. The Morávka meteorite fall: I. Description of the events and determination of the fireball trajectory and orbit from video records. *Meteoritics & Planetary Science* 38:975–987.

Borovička J. and Spurný P. 1996. Radiation study of two very bright terrestrial bolides and an application to the comet S-L 9 collision with Jupiter. *Icarus* 121:484–510.

Bottke W. F., Jr., Jedicke R., Morbidelli A., Petit J.-M., and Gladman B. 2000. Understanding the distribution of near-Earth asteroids. *Science* 288:2190–2194.

Bottke W. F., Jr., Morbidelli A., Jedicke R., Petit J.-M., Levison H. F., Michel P., and Metcalfe T. S. 2002. Debiased orbital and absolute magnitude distribution of the near-Earth objects. *Icarus* 156: 399–433.

Bottke W. F., Jr., Morbidelli A., and Jedicke R. 2004. Recent progress in interpreting the nature of the near-Earth object population. In *Mitigation of hazardous comets and asteroids*, edited by Belton M. J. S., Morgan T. H., Samarasinha N. H., and Yeomans D. K. Cambridge: Cambridge University Press. pp. 1–21.

Brown P. G., Ceplecha Z., Hawkes R. L., Wetherill G., Beech M., and Mossman K. 1994. The orbit and atmospheric trajectory of the Peekskill meteorite from video records. *Nature* 367:624–626.

Brown P., Hildebrand A. R., Green D. W. E., Page D., Jacobs C., ReVelle D., Tagliaferri E., Wacker J., and Wetmiller B. 1996. The fall of the St-Robert meteorite. *Meteoritics & Planetary Science* 31:502–517.

Brown P. G., Spalding R. E., ReVelle D. O., Tagliaferri E., and Worden S. P. 2002a. The flux of small near-Earth objects colliding with the Earth. *Nature* 420:294–296.

Brown P. G., ReVelle D. O., Tagliaferri E., and Hildebrand A. R. 2002b. An entry model for the Tagish Lake fireball using seismic, satellite, and infrasound records. *Meteoritics & Planetary Science* 37:661–675.

Brown P. G., Pack D., Edwards W. N., ReVelle D. O., Yoo B. B., Spalding R. E., and Tagliaferri E. 2004 The orbit, atmospheric dynamics, and initial mass of the Park Forest meteorite. *Meteoritics & Planetary Science* 39:1781–1796.

Carusi A., Valsecchi G., D'Abramo G., and Boattini A. 2002. Deflecting NEOs in route of collision with the Earth. *Icarus* 159: 417–422.

Ceplecha Z. 1961. Multiple fall of Pribam meteorites photographed. *Bulletin of the Astronomical Institute of Czechoslovakia.* 12:21–47.

Ceplecha Z. 1996. Luminous efficiency based on photographic observations of the Lost City fireball and implications on the influx of interplanetary bodies onto Earth. *Astronomy & Astrophysics* 279:329–332.

Ceplecha Z., Borovička J., Elford G. W., ReVelle D. O., Hawkes R. L., Porubčan V., and Šimek M. 1998. Meteor phenomena and bodies. *Space Science Reviews* 84:327–471.

Di Martino M. and Cellino A. 2004. Physical properties of comets and asteroids inferred from fireball observations. In *Mitigation of hazardous comets and asteroids*, edited by Belton M. J. S., Morgan T. H., Samarasinha N. H., and Yeomans D. K. Cambridge: Cambridge University Press. pp. 153–166.

Fesenkov V. G. 1951. The Sikhote-Alin meteorite fall. *Meteoritika* 9: 27. In Russian.

Folinsbee R. E., Bayrock L. A., Cumming G. L., and Smith D. G. W. 1969. Vilna Meteorite-Camera: Visual, seismic, and analytic records (abstract). *Journal of the Royal Astronomical Society of Canada* 72:61.

Gladman B. J., Migliorini F., Morbidelli A., Zappala V., Michel P., Cellino A., Froeschle C., Levison H. F., Bailey M., and Duncan M. 1997. Dynamical lifetimes of objects injected into asteroid belt resonances. *Science* 277:197–201.

Gounelle M., Spurný P., and Bland P. A. 2006. The orbit and atmospheric trajectory of the Orgueil meteorite from historical records. *Meteoritics & Planetary Science* 41:135–150.

Grady M. M. 2000. *Catalogue of meteorites*, 5th ed. Cambridge: Cambridge University Press. 670 p.

Halliday I., Blackwell A. T., and Griffin A. A. 1978. The Innisfree meteorite and the Canadian camera network. *Journal of the Royal Astronomical Society of Canada* 72:15–39.

Halliday I. and McIntosh B. 1990. Orbit of the Murchison meteorite. *Meteoritics* 25:339–340.

Halliday I., Griffin A. A., and Blackwell A. T. 1996. Detailed data for 259 fireballs from the Canadian camera network and inferences concerning the influx of large meteoroids. *Meteoritics & Planetary Science* 31:185–217.

Jenniskens P., Borovička J., Betlem H., ter Kuile C., Bettonvil F., and Heinlein D. 1992. Orbits of meteorite producing fireballs: The Glanerbrug—A case study. *Astronomy & Astrophysics* 255:373–376.

Krinov E.L. 1960. *Principles of meteorites*. New York: Pergamon Press. 208 p.

La Paz L. 1949. The achondritic shower of February 18, 1948. *Publications of the Astronomical Society of the Pacific* 61:63.

Levin B. J., Simonenko A. N., and Anders E. 1976. Farmington meteorite: A fragment of an Apollo asteroid. *Icarus* 28:307–324.

Llorca J., Trigo-Rodríguez J. M., Ortiz J. L., Docobo J. A., García-Guinea J., Castro-Tirado A. J., Rubin A. E., Eugster O., Edwards W., Laubenstein M., and Casanova I. 2005. The Villalbeto de la Peña meteorite fall: I. Fireball energy, meteorite recovery, strewn field, and petrography. *Meteoritics & Planetary Science* 40:795–804.

McCrosky R. E., Posen A., Schwartz G., and Shao C.-Y. 1971. The Lost City meteorite: Its recovery and a comparison with other fireballs. *Journal of Geophysical Research* 76:4090–4108.

Morbidelli A. and Gladman B. 1998. Orbital and temporal distributions of meteorites originating in the asteroid belt. *Meteoritics & Planetary Science* 33:999–1016.

Rabinowitz D. L., Gehrels T., Scotti J. V., McMillan R. S., Perry M. L., Winslewski W., Larson S. M., Howel E. S., and Mueller E. A. 1993. Evidence for a near-Earth asteroid belt. *Nature* 363: 704–706.

Rabinowitz D. L., Helin E., Lawrence K., and Pravdo S. 2000. A reduced estimate of the number of kilometre-sized near-Earth asteroids. *Nature* 403:165–166.

Spurný P., Oberst J., and Heinlein D. 2003. Photographic observations of Neuschwanstein, a second meteorite from the orbit of the Přibram chondrite. *Nature* 423:151–153.

Steel D. 1996. Meteoroid orbits. *Space Science Reviews* 78:507–553.

Stuart J. S. and Binzel R. P. 2004. Bias-corrected population, size distribution, and impact hazard for the near-Earth objects. *Icarus* 170:295–311.

Vokrouhlický D. and Farinella P. 2000. Efficient delivery of meteorites to the Earth from a wide range of asteroid parent bodies. *Nature* 407:606–608.

Wisdom J. 1985a. Meteorites may follow a chaotic route to Earth. *Nature* 315:731–733.

Wisdom J. 1985b. A perturbative treatment of motion near the 3/1 commensurability. *Icarus* 63:272–289.

Wylie C. C. 1948. The orbits of three stone-dropping meteors. *Popular Astronomy* 56:144.